

# Multirate Obstacle Tracking and Path Planning for Intelligent Vehicles

Marta C. Mora, Ricardo Pizá and Josep Tornero, *Member, IEEE*

**Abstract**— This paper introduces a new approach for tracking and path planning for intelligent vehicles. The tracking application takes into account the trajectories followed by the obstacles, making a prediction of their future positions and corresponding uncertainties. This idea introduces a stochastic model for obstacle and vehicle kinematics. A multi-rate Kalman filter is considered in the tracking process in order to manage the uncertainty. Potential Field approach for path planning is redefined according to the new stochastic models. In particular, the repulsive potential field is modified to consider these models projected into a prediction horizon. The use of future information minimizes the risk of collisions and generates smoother trajectories.

## I. INTRODUCTION

PATH planning applications in intelligent vehicles require gathering information of the environment for solving the problem of generating free-collision trajectories. Several applications use a map of the environment for their calculations. In general, the environment is dynamic where mobile obstacles (targets) are present. Identifying targets and tracking their trajectories increases the performance of path planning algorithms.

In the literature [1, 2, 3, 4, 5] target tracking mainly covers ballistic problems using filtering techniques such as Kalman filtering or its successors, for example alpha beta or alpha beta gamma trackers.

Reactive path planning approaches deal properly with unstructured and dynamic environments. Examples of these methods include: Potential Fields methods [6], Vector Field Histogram [7, 8], Elastic Bands [9], Elastic Strips [10], Nearness Diagram Navigation [11, 12], the Curvature-Velocity Method [13] and the Dynamic Window approach [14, 15].

Some of the most popular reactive methods are based on Artificial Potential Fields [6]. In them, the vehicle steering direction is determined assuming that obstacles generate repulsive forces and the goal generates attractive forces on the vehicle. These methods are extremely fast when considering just a small subset of obstacles near the vehicle.

In this paper, target tracking and reactive path planning are considered simultaneously. Once a target is identified, several tasks are performed: path - tracking, uncertainty

evaluation, future position prediction and path planning. The final result of the tracking is a map of uncertainty areas combining present and future time instants which generates a potential field.

This paper presents a new adaptation to the classical Potential Fields technique that uses the previous map, considering the effect of future positions and uncertainties in the computation of repulsive forces.

The paper is organized as follows: next section focuses on path tracking application; section III describes the Potential Field Projection approach; section IV presents some experimental and simulation results and finally section V are the conclusions.

## II. PATH TRACKING APPLICATION

The set of algorithms included in the path tracking application follow the stages listed below:

- 1) Target detection and characterization.
- 2) Target list management.
- 3) Target path tracking.
- 4) Evaluation of target estimation.
- 5) Calculus of target influence area.

### A. Target Detection and Characterization

Application design requirements are:

- Number of targets in the environment is unknown when application starts.
- Number of targets is dynamic, new targets must be detected and tracked while application runs.
- Support temporal disappearance of targets.

We assume that a geometric environment map is available which, for simplicity, only contains lines and arcs. This map is easy to use and has low computational requirements; therefore processing capacity is still available for other applications.

Mobile obstacles (targets) appear in the map as a set of geometric entities separate from walls. When a shape with these characteristics is detected, it is analyzed to verify whether or not it is a mobile obstacle.

The geometric representation for pedestrians is simplified with a small diameter circle. For vehicles, bigger than pedestrians, their simplified geometry is a circle hull which envelopes the obstacle.

Target detection process provides a list of possible targets. For each one, position (center of circle), size (radius) and target type (pedestrian or vehicle) is obtained and stored.

M.C. Mora is with the Mechanical Engineering and Construction Department, Jaume I University, Spain (corresponding author to provide phone: +34 964 72 81 26; e-mail: [mmora@emc.uji.es](mailto:mmora@emc.uji.es)).

R. Pizá and J. Tornero are with the Systems Engineering and Control Department, Technical University of Valencia, Spain.

When a target is tracked, estimation data includes target position and speed together with their uncertainty level.

### B. Target List Management

For every iteration of the algorithm we obtain a list of possible mobile obstacles extracted from the geometric map. This list is compared with the existing list of targets which have been tracked. Thus, positions will be updated and new targets will be detected. The set of operations to do at this stage is:

- 1) Target matching and position updating.
- 2) Target creation for new obstacles.
- 3) Target removal for old hidden obstacles.

Matching is necessary for determining whether or not the detected obstacles correspond to tracked targets. Detected objects are compared with targets considering position and size: object position with target uncertainty ellipsoid and object radius with target radius. A mobile object is matched with a target when the mobile object position is in the target uncertainty ellipsoid and their radii are comparable.

Fig. 1 shows the matching process. Targets are represented by their uncertainty ellipsoids and detected mobile obstacles by dots. Uncertainty ellipsoids of matched targets contain a dot corresponding to a detected object.

Matched targets are “visible” because an observation of their position is available. Otherwise unmatched targets are “hidden” and become candidates to be removed from the list, depending on an index evaluation (see subsection D). Finally, unmatched objects (new targets) are appended to the list of targets. This process is shown in Fig. 2.

Target list includes *target position observation* (only available for matched targets) and *target position estimation*. New targets generate a new estimation initialized to the target position observation.

Target tracking is carried out using Kalman filtering where associated matrices (system and filter matrices) are in diagonal blocks depending on the number of targets, as described below.

### C. Target Path Tracking

Dynamic models of moving targets are essential in the estimation procedure. In this sense, two different model approximations for pedestrians and vehicles have been considered.

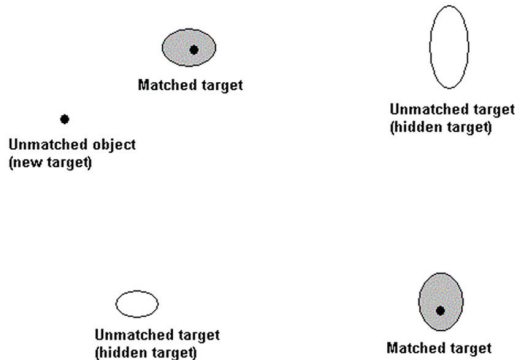


Fig. 1 Matching process representation.

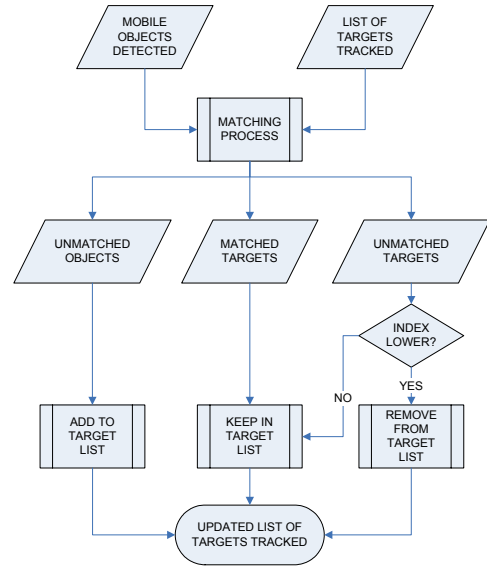


Fig. 2 Target list management process.

Pedestrian targets are modeled as moving particles where the state vector is composed of target position and target speed in XY coordinates. Using Euler approximation, this model corresponds to the following equations:

$$\begin{bmatrix} x \\ y \\ v_x \\ v_y \end{bmatrix}_{k+1} = \begin{bmatrix} 1 & 0 & T & 0 \\ 0 & 1 & 0 & T \\ 0 & 0 & 1 & 0 \\ 0 & 0 & 0 & 1 \end{bmatrix} \begin{bmatrix} x \\ y \\ v_x \\ v_y \end{bmatrix}_k + \begin{bmatrix} \frac{T^2}{2} & 0 \\ 0 & \frac{T^2}{2} \\ T & 0 \\ 0 & T \end{bmatrix} \begin{bmatrix} a_x \\ a_y \end{bmatrix} \quad (1)$$

$$\begin{bmatrix} \tilde{x} \\ \tilde{y} \end{bmatrix}_k = \begin{bmatrix} 1 & 0 & 0 & 0 \\ 0 & 1 & 0 & 0 \end{bmatrix} \begin{bmatrix} x \\ y \\ v_x \\ v_y \end{bmatrix}_k \quad (2)$$

Vehicle targets are modeled with non-linear equations taking into account vehicle kinematics. While pedestrians usually describe lines in their trajectory and changes of direction are made suddenly as breakpoints, vehicles describe a curve trajectory due to their kinematical restrictions (links between straight lines must be curves). The corresponding dynamic model for vehicle targets is described in (3) and (4).

It can be seen that only two states can be observed. This is because it is practically impossible to measure target orientation based only on sensor distance measures.

$$\begin{bmatrix} x \\ y \\ \varphi \\ V_C \\ \omega_C \end{bmatrix}_{k+1} = \begin{bmatrix} 1 & 0 & 0 & T \cdot \cos\varphi & 0 \\ 0 & 1 & 0 & 0 & T \cdot \sin\varphi \\ 0 & 0 & 1 & 0 & T \\ 0 & 0 & 0 & 1 & 0 \\ 0 & 0 & 0 & 0 & 1 \end{bmatrix} \begin{bmatrix} x \\ y \\ \varphi \\ V_C \\ \omega_C \end{bmatrix}_k + \begin{bmatrix} \frac{T^2 \cdot \cos\varphi}{2} & 0 \\ \frac{T^2 \cdot \sin\varphi}{2} & 0 \\ 2 & 0 \\ 0 & \frac{T^2}{2} \\ T & 0 \\ 0 & T \end{bmatrix} \begin{bmatrix} a_C \\ \alpha_C \end{bmatrix} \quad (3)$$

$$\begin{bmatrix} \tilde{x} \\ \tilde{y} \end{bmatrix}_k = \begin{bmatrix} 1 & 0 & 0 & 0 & 0 \\ 0 & 1 & 0 & 0 & 0 \end{bmatrix} \begin{bmatrix} x \\ y \\ \varphi \\ V_C \\ \omega_C \end{bmatrix}_k \quad (4)$$

Tracking a single object at low speed is a simple process which can be implemented using single-rate filtering techniques. When many targets are involved and/or moving at high speed, single-rate filtering at high frequency cannot be implemented. However, Euler approximation used in dynamic models requires high frequencies. Therefore, multirate techniques must be applied.

Many multirate models can be found in the literature. In this paper we use a dynamic multirate system model [16, 17, 18] as shown in (5),

$$\begin{bmatrix} x_{k+1} \\ u_{k+1}^u \\ u_{k+1}^v \\ u_k \\ y_k \end{bmatrix} = \begin{bmatrix} A_{SR}(T) & B_{SR}(T)(I - \Delta_k^u) & 0 & B_{SR}(T) \cdot \Delta_k^u & 0 \\ 0 & I - \Delta_k^u & 0 & \Delta_k^u & 0 \\ \Delta_k^v C_{SR}(T) & 0 & I - \Delta_k^v & \Delta_k^v D_{SR}(T) & 0 \\ 0 & 0 & 0 & I & 0 \\ \Delta_k^v \cdot C_{SR}(T) & \Delta_k^v D_{SR}(T)(I - \Delta_k^v) & I - \Delta_k^v & \Delta_k^v D_{SR}(T) \Delta_k^u & 0 \end{bmatrix} \begin{bmatrix} x_k \\ v_k^u \\ v_k^v \\ u_k \\ y_k \end{bmatrix} \quad (5)$$

where state space multirate matrices are obtained from previous matrices and  $\Delta_k^u$ ,  $\Delta_k^v$  are the sampling matrices defined in [17].

$$A_{MR_{k,T}} = \begin{bmatrix} A_{SR}(T) & B_{SR}(T)(I - \Delta_k^u) & 0 \\ 0 & I - \Delta_k^u & 0 \\ \Delta_k^v C_{SR}(T) & 0 & I - \Delta_k^v \end{bmatrix} \quad B_{MR_{k,T}} = \begin{bmatrix} B_{SR}(T) \Delta_k^u \\ \Delta_k^u \\ \Delta_k^v D_{SR}(T) \end{bmatrix} \quad (6)$$

$$C_{MR_{k,T}} = [\Delta_k^v C_{SR}(T) \quad \Delta_k^v D_{SR}(T)(I - \Delta_k^v) \quad I - \Delta_k^v] \quad D_{MR_{k,T}} = [\Delta_k^v D_{SR}(T) \Delta_k^u]$$

Applying this formulation, a multirate system model of a target can be obtained for either a pedestrian model (1, 2) or a vehicle model (3, 4). According to these multirate models, two multirate Kalman filters have been proposed. A linear Kalman filter, applied to pedestrian targets, expressed as follows:

$$P_{0/0} = \begin{bmatrix} Var(X_0) \\ 0 \end{bmatrix} \quad \hat{X}_{0/0} = \begin{bmatrix} E(X_0) \\ 0 \end{bmatrix}$$

$$\begin{aligned} P_{MR_{k/k-1}} &= \overbrace{A_{MR_{k-1,T}} \cdot P_{MR_{k-1/k-1}} \cdot A_{MR_{k-1,T}}^T + \Gamma_{MR_{k-1,T}} \cdot Q_k \cdot \Gamma_{MR_{k-1,T}}^T}^{\text{for } i=1,2,\dots} \\ K_{MR_k} &= P_{MR_{k/k-1}} \cdot C_{MR_{k-1,T}}^T \cdot (C_{MR_{k-1,T}} \cdot P_{MR_{k/k-1}} \cdot C_{MR_{k-1,T}}^T + R_k)^{-1} \cdot \Delta_k \quad (7) \\ P_{MR_{k/k}} &= P_{MR_{k/k-1}} - K_{MR_k} \cdot C_{MR_{k-1,T}} \cdot P_{MR_{k/k-1}} \\ \hat{X}_{k/k-1} &= A_{MR_{k-1,T}} \cdot \hat{X}_{k-1/k-1} + B_{MR_{k-1,T}} \cdot u_k \\ \hat{X}_{k/k} &= \hat{X}_{k/k-1} + K_{MR_k} (v_k - C_{MR_{k,T}} \cdot \hat{X}_{k/k-1} - D_{MR_{k,T}} \cdot u_k) \end{aligned}$$

and an extended Kalman filter applicable to the non-linear model of the vehicle, developed in (8).

$$P_{(0/0)} = Var \begin{bmatrix} Var(X_0) \\ 0 \end{bmatrix} \quad \hat{X}'_{0/0} = \begin{bmatrix} X \\ v \end{bmatrix}_{0/0} = \begin{bmatrix} E(X_0) \\ 0 \end{bmatrix}$$

$$\begin{aligned} P_{k/k-1} &= \overbrace{\frac{\partial g'_{k-1}}{\partial X'} \bigg|_{\hat{X}'_{k-1/k-1}} \cdot P_{k-1/k-1} \cdot \frac{\partial g'_{k-1}}{\partial X'} \bigg|_{\hat{X}'_{k-1/k-1}}^T + H'_{k-1} \bigg|_{X'_{k-1/k-1}} Q_{k-1} H'_{k-1} \bigg|_{\hat{X}'_{k-1/k-1}}^T}^{\text{for } i=1,2,\dots} \\ K_k &= P_{k/k-1} \cdot \frac{\partial g'_{k-1}}{\partial X'} \bigg|_{\hat{X}'_{k-1/k-1}}^T \cdot \left( \frac{\partial g'_{k-1}}{\partial X'} \bigg|_{\hat{X}'_{k-1/k-1}} \cdot P_{k/k-1} \cdot \frac{\partial g'_{k-1}}{\partial X'} \bigg|_{\hat{X}'_{k-1/k-1}}^T + R_k \right)^{-1} \cdot \Delta_k \quad (8) \\ P_{k/k} &= P_{k/k-1} - K_k \cdot \frac{\partial g'_{k-1}}{\partial X'} \bigg|_{\hat{X}'_{k-1/k-1}} \cdot P_{k/k-1} \\ \hat{X}'_{k/k-1} &= f'_{k-1}(\hat{X}'_{k-1}) \\ \hat{X}'_{k/k} &= \hat{X}'_{k/k-1} + K_k (v_k - g'_k(\hat{X}'_{k/k-1})) \end{aligned}$$

The tracking procedure is implemented in two separate processes, one for linear and another for non-linear tracking.

In the linear estimation process pedestrian targets are considered in a distributive structure. In this structure, estimation is carried out using block diagonal matrices, where each block corresponds to one pedestrian as shown in (9) and (10). In the same way, non-linear estimation process for vehicle targets also uses a distributive structure.

$$A = diag(A_1, A_2, \dots, A_n) \quad B = diag(B_1, B_2, \dots, B_n) \\ C = diag(C_1, C_2, \dots, C_n) \quad D = diag(D_1, D_2, \dots, D_n) \quad (9)$$

$$P = diag(P_1, P_2, \dots, P_n) \quad \Gamma = diag(\Gamma_1, \Gamma_2, \dots, \Gamma_n) \\ Q = diag(Q_1, Q_2, \dots, Q_n) \quad R = diag(R_1, R_2, \dots, R_n) \quad (10)$$

State vector and covariance matrices inherit the same distributive structure. Each block in the covariance matrix P contains on its own diagonal the variances of estimated variables. Using this information, an uncertainty ellipsoid centered on the estimated position, can be constructed. This ellipsoid represents the region inside which the target is most likely to be located.

When target measures are available the uncertainty ellipsoid decreases, otherwise the ellipsoid grows.

Fig. 3 shows a representation of tracking for a pedestrian (top side) and a vehicle (bottom side) target type. Due to the particle model characteristics, uncertainty ellipsoids become circles for the pedestrian. We can also observe that if target observations are not available the ellipsoid area increases (shaded zones), modeling the growth of uncertainty in target position estimation.

#### D. Evaluation of Target Estimation

Each target position estimation obtained can be evaluated using its correspondent covariance sub-matrix.

Although the entire target list is embedded in a dynamic model defined with the appropriate matrices, the list can be separated into their decoupled component subsystems. For each one of these subsystems, the diagonal of the sub-matrix P contains information on estimation noise variances. Processing this information generates an uncertainty ellipsoid representing the uncertainty area where target must be located.

Evolution of P depends on availability of measurements taken along the filtering process and characteristic noise system sub-matrices Q and R. Matrix P has an optimum characteristic value corresponding to the equivalent single rate Kalman filter. Each time a target position measurement is not available, uncertainty estimation increases, with this effect being reflected in the matrix P.

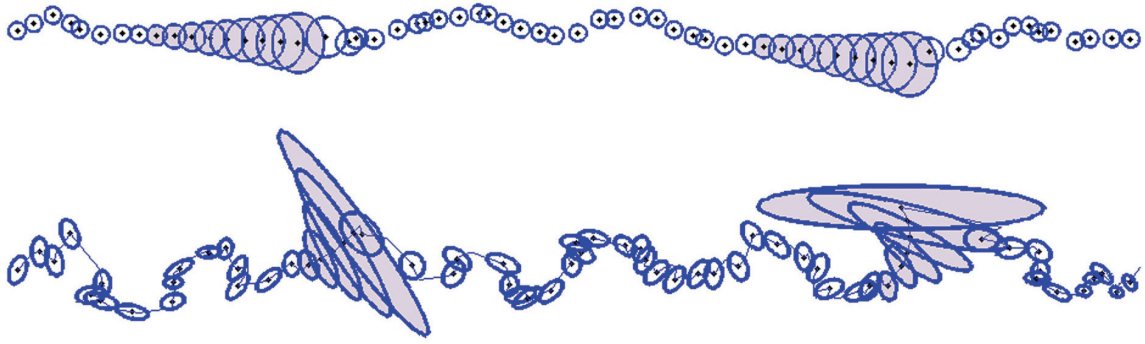


Fig. 3 Tracking of a pedestrian (top figure) and a vehicle (bottom figure). Shaded zones represent instants without measurement.

Applying this idea, the estimates obtained can be compared with optimum estimates defining an *estimation quality index* in the form:

$$J = \exp\left(-\frac{(\text{trace}(\mathbf{P}) - \text{trace}(\hat{\mathbf{P}}_{\text{optim}}))^2}{\sigma}\right) \quad (11)$$

Where  $\mathbf{P}_{\text{optim}}$  is the  $\mathbf{P}$  matrix obtained off line for the corresponding single-rate equivalent system and  $\sigma$  is a user adjustable distribution scaling factor.

Depending on the measure sequence index, evaluation varies between a maximum level of one and zero. A high level index evaluation means a good estimation while a low level index evaluation means a poor estimation with considerable uncertainty. Fig. 4 shows index evolution with unavailability of measures of the obstacle position.

As shown in this figure, in complete absence of measurements, the index continuously decreases. If measurements are available, index increases breaking with plot tendency.

If the index rises to value 1, the estimation obtained corresponds to a possible optimum. If the index value decreases, it is due to the absence of measurements, sometimes due to multirate nature of the process and other times because the object is hidden.

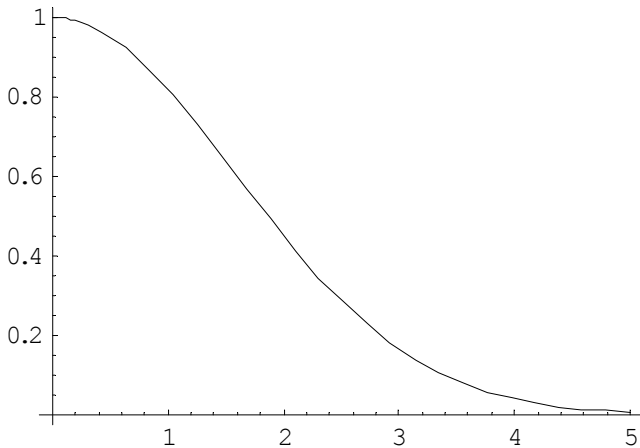


Fig. 4 Plot of the estimation quality index against absence of measures.

Therefore, if measurements are not available for a long time, uncertainty increases to higher levels and the index decreases considerably. In these circumstances, the index value is used as a measure of estimation quality, and considered in other tasks such as path planning.

Moreover, if the index decreases under a threshold limit value  $J_{\text{min}}$ , fixed by user, it means the continuous absence of target measurements for a long time and increasing of uncertainty to excessive high values. When this situation occurs, the target is removed from the list of targets and all its data are deleted. This is the condition to remove a target as explained previously in “target list management”.

#### E. Calculus Of Target Influence Area

A particular application of path tracking is trajectory prediction by projecting the present trajectory. Using the filter equations, the target trajectory can be projected in time making a prediction of the future target evolution. As the calculations made are a prediction, they are affected by a considerable uncertainty level that grows with projection. This characteristic is used in the path planning application.

A trajectory prediction consists of running filter equations without measurements available for a set of “future sampling times”, which becomes a trajectory projection. Therefore, during the projection, as measurements are not available,  $\Delta$  matrices are zero for the entire prediction horizon and it is only necessary to run the equations (12) for pedestrian targets and (13) for vehicle targets.

$$P_{MR_{k/k-1}} = A_{MR_{k-1,T}} \cdot P_{MR_{k-1/k-1}} \cdot A_{MR_{k-1,T}}^T + \Gamma_{MR_{k-1,T}} \cdot Q_k \cdot \Gamma_{MR_{k-1,T}}^T \quad (12)$$

$$\hat{X}_{k/k-1} = A_{MR_{k-1,T}} \cdot \hat{X}_{k-1/k-1} + B_{MR_{k-1,T}} \cdot u_k$$

$$P_{k/k-1} = \frac{\partial f'_{k-1}}{\partial X^1} \Big|_{\hat{X}_{k-1/k-1}} \cdot P_{k-1/k-1} \cdot \frac{\partial f'_{k-1}}{\partial X^1} \Big|_{\hat{X}_{k-1/k-1}}^T + H'_{k-1} \Big|_{X_{k-1/k-1}} \cdot Q_{k-1} \cdot H'_{k-1} \Big|_{\hat{X}_{k-1/k-1}}^T \quad (13)$$

$$\hat{X}'_{k/k-1} = f'_{k-1}(\hat{X}'_{k-1})$$

As projection means unavailability of measures, as long as predictions are made, uncertainty of prediction increases. In this sense, Fig. 5a shows the uncertainty ellipsoid evolution in trajectory projection for two pedestrian targets with a projection horizon of 5 seconds. The evolving area defined by the set of ellipsoids is called the *target influence area*.

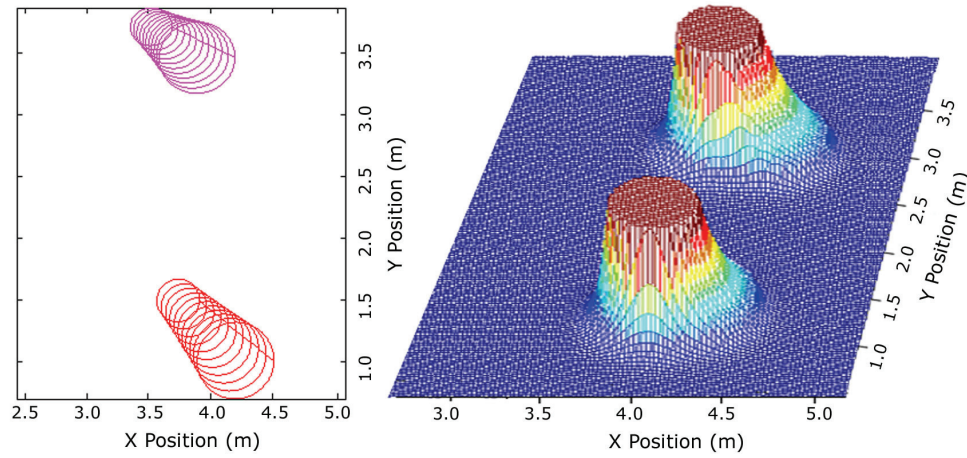


Fig. 5 a) Projected uncertainty ellipsoids of two obstacles (left), b) Repulsive potential field (right).

### III. PATH PLANNING USING POTENTIAL FIELD PROJECTION

The concepts explained in previous sections have been used for developing a new path planning approach based on Artificial Potential Fields [6]. In this sense, the target influence areas corresponding to all tracked targets are considered as restricted areas for path planning and must be avoided to minimize the risk of collision. The intelligent vehicle influence area and the obstacles influence areas should not collide to ensure collision-free movements.

In particular, we have considered that every ellipsoid obtained from obstacles trajectory projection only has influence on the corresponding vehicle ellipsoid, i.e, only ellipsoids obtained in the same sample time are tested for possible collisions.

In order to reflect the influence of the trajectory projection in the path planning algorithm, the repulsive potential function is defined as shown in the following equation:

$$U_{rep}(q,i) = \begin{cases} \frac{1}{2} \eta J^i \left( \frac{1}{MTD_i} - \frac{1}{\rho_0} \right)^2 & \text{if } MTD_i \leq \rho_0 \\ 0 & \text{if } MTD_i > \rho_0 \end{cases} \quad (14)$$

where  $J \in [0, 1]$  is the estimation quality index and  $i \in [0, N]$  indicates the number of instants after the last measurement was done, being  $N$  the number of ellipsoids that generate the influence area.  $N$  is determined from the temporal projection horizon  $\Delta T$  and the estimation period  $T$  as  $N = \Delta T / T$ .  $\rho_0$  represents the limit distance of the repulsive potential field influence and  $MTD_i$  is the minimum translational distance between the vehicle and the obstacle in the  $i$ -th projection instant. The Minimum Translational Distance is defined in [19] as the shortest relative translation of two models to bring them in contact. In this way, when two models are not intersecting, MTD represents the separation distance between them. Otherwise if models are colliding, MTD states the penetration distance. Depending on the values of MTD we can distinguish between different collision situations, as detailed in Table I.

The estimation quality index  $J$  quantifies the reliability of the estimation. It depends on the precision and uncertainty of the sensors employed. Therefore, the influence of the repulsive potential field for future instants depends on the quality of the estimation, as shown in (14).

The factor  $J^i$  causes a degradation of the potential field in the sense that as  $i$  grows (the instant considered moves away from the last measure instant), the probability that the obstacle follows the estimated trajectory decreases. This situation leads to a “vanishing” of the potential field as time goes by without sensor information. An example of the evolution of the repulsive potential field in a dynamic environment, considering a vehicular environment with two mobile obstacles, is shown in Fig. 5b.

The repulsive potential field obtained before generates a repulsive force applied to the vehicle defined as

$$F_{rep}(q,i) = -\nabla U_{rep}(q,i)$$

$$\vec{F}_{rep}(q,i) = \begin{cases} \eta J^i \left( \frac{1}{MTD_i} - \frac{1}{\rho_0} \right) \frac{1}{MTD_i^2} \vec{u}_{MTD_i} & \text{if } MTD_i \leq \rho_0 \\ 0 & \text{if } MTD_i > \rho_0 \end{cases} \quad (15)$$

where  $\vec{u}_{MTD_i}$  is a unit vector in the direction of  $MTD_i$ . The total repulsive force generated by all the obstacles is:

$$\vec{F}_{rep}(q,i) = \sum_{k=1}^r \vec{F}_{rep_k}(q,i) \quad (16)$$

where the repulsive force magnitude decreases as  $i$  grows.

We have obtained a set of repulsive forces that, applied on the intelligent vehicle in successive instants, generates a continuous avoiding movement of the robot during the projection horizon, as shown in Fig. 6.

TABLE I  
COLLISION SITUATIONS

$MTD_i$	Situation
$MTD_i > \rho_0$	No avoidance
$MTD_i = \rho_0$	Starting avoidance
$MTD_i \leq \rho_0$	Avoidance
$MTD_i = 0$	Avoidance (Contact)

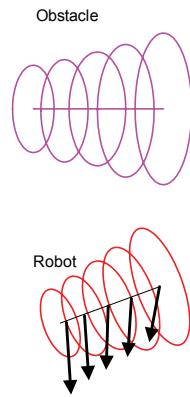


Fig. 6 Repulsive forces obtained from the potential field projection.

IV. SIMULATIONS AND EXPERIMENTAL RESULTS

Some simulations have been developed to show the performance of the Potential Field Projection approach for particle model environments.

In Fig. 7 the intelligent vehicle uncertainty ellipses avoid the obstacles uncertainty ellipses. These ellipsoids are derived from the potential field projection. At the beginning of the simulation, the mobile robot moves along a straight line. As the upper obstacle comes closer to the vehicle, it starts a smooth avoiding maneuver that modifies its initial trajectory.

A set of experiments has been developed to verify target tracking application using an electric vehicle as development platform and other vehicles and pedestrians as targets. Our development platform is a vehicle equipped with distance sensors, laser scanner, ultrasonic and infrared sensors.

V. CONCLUSIONS

This paper introduces a new approach for tracking and path planning in dynamic environments by combining Kalman filtering and Artificial Potential Fields.

Traditional artificial potential fields considers deterministic positions for obstacles and vehicles at a given instant of time. However, the present proposal also considers position uncertainties of obstacles and vehicles at the present instant as well as in future instants of time within a temporal horizon.

Using Kalman filter equations, obstacles trajectories are computed making a prediction of future positions and uncertainties. These uncertainties grow with time.

Two different kinematic models have been considered in Kalman filtering for moving targets: particles for pedestrians and non-linear kinetics for vehicles.

Missing data and low speed sensor acquisition have been supported using multirate models considered in Kalman Filter. In this technique the number of targets to be tracked is completely dynamic allowing targets to appear and disappear at any time.

It is interesting to remark that by introducing Kalman filtering into path planning a most powerful collision avoidance technique has been obtained.

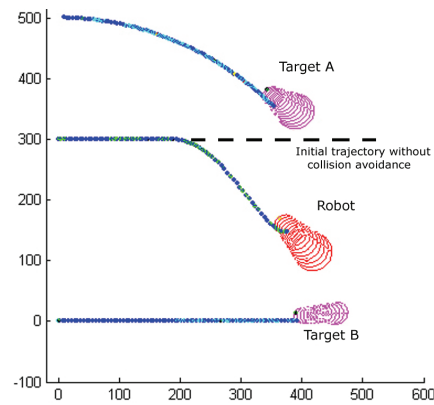


Fig. 7 Obstacle avoidance using Potential Field Projection approach.

VI. REFERENCES

- [1] Y. Bar-Shalom and X. Li, *Multitarget Multisensor Tracking: Principles and Techniques*, YBS publishing, 1995.
- [2] Y. Bar Shalom and X. Li, *Estimation and Tracking: Principles, Techniques and Software*, YBS publishing, 1998.
- [3] S. Blackman, *Multiple Target Tracking with Radar Applications*, Artech House, 1986.
- [4] E. Brookner, *Tracking and Kalman Filtering Made Easy*, Wiley Interscience, 1998.
- [5] C.K. Chui, G. Chen, *Kalman Filtering with Real-Time Applications*, Springer Verlag, 1987.
- [6] O. Khatib, "Real-time obstacle avoidance for manipulators and mobile robots," *The Int. Journal of Robotics Research*, vol. 5, n° 1, pp. 90-98, 1986.
- [7] J. Borenstein and Y. Koren, "The Vector Field Histogram - Fast obstacle avoidance for mobile robots," *IEEE Transactions on Robotics and Automation*, vol. 7, no. 3, pp.278-287, 1991.
- [8] I. Ulrich and J. Borenstein, "VFH\*: Local obstacle avoidance with look-ahead verification," *IEEE International Conference on Robotics and Automation*, pp. 2505-2511, 2000.
- [9] S. Quinlan and O. Khatib, "Elastic Bands: Connecting path planning and control," *IEEE International Conference on Robotics and Automation*, vol. 2, pp. 802-807, 1993.
- [10] O. Brock and O. Khatib, "Real-time replanning in high-dimensional configuration spaces using sets of homotopic paths," *IEEE Int. Conf. Robotics and Automation*, pp. 2328-2334, 2000.
- [11] J. Minguez and L. Montano, "Nearness Diagram navigation (ND): a new real time collision avoidance approach," *IEEE/RSJ Int. Conf. on Intelligent Robots and Systems*, pp. 2094-2100, 2000.
- [12] J. Minguez, L. Montano, "Nearness Diagram Navigation (ND): Collision Avoidance in Troublesome Scenarios," *IEEE Transactions on Robotics and Automation*, vol. 20, no. 1, pp. 45-59, 2004.
- [13] R. Simmons, "The Curvature-Velocity Method for local obstacle avoidance," *IEEE International Conference on Robotics and Automation*, pp. 3375-3382, 1996.
- [14] D. Fox, W. Burgard and S. Thrun, "The Dynamic Window approach to collision avoidance," *IEEE Robotics and Automation Magazine*, vol. 4, no.1, pp.23-33, 1997.
- [15] P. Ögren and N.E. J. Leonard, "A convergent dynamic window approach to obstacle avoidance," *IEEE Transactions on Robotics*, vol. 21, no. 2, pp. 188-195, 2005
- [16] R. Pizá, *Modelado del entorno y localización de robots móviles autónomos mediante técnicas de muestreo no convencional*, (in spanish), Ph. D. Thesis, Politechnic University of Valencia, 2003.
- [17] J. Tornero, R. Pizá, P. Albertos and J. Salt. "Multirate LQG controller applied to self-location and path-tracking in mobile robots". *IEEE/RSJ Int. Conf. Intelligent Robots and Systems*, 2001.
- [18] R. Piza, J. Tornero and M. Tomizuka, "Self-localization and path-tracking in mobile robots. Dual-rate Kalman filtering", *System Identification and Control Problems*, 2000.
- [19] E. J. Bernabeu and J. Tornero, "Hough transform for distance computation and collision avoidance", *IEEE Transactions on Robotics and Automation*, vol. 18, no. 3, pp. 393-398, 2002.